Enhanced Multi-Resolution Hierarchical Codebook Design for Adaptive Compressed Sensing Based Millimeter Wave Channel Estimation

Jianyi Yang, Zaixue Wei, Nanxi Li, Lin Sang and Pengxiang Li
School of Information and Communication Engineering, Beijing University of Posts and Telecommunications
Email: {yangjianyi, zaixuew, airnanxil, sanglin}@bupt.edu.cn

***Abstract*—Perfect channel state information (CSI) is essential for precoding and combining in millimeter wave (mmWave) systems. The CSI estimation algorithm based on adaptive compressed sensing (CS) is an efficient method. However, the imperfect multi-resolution hierarchical codebook design possibly leads to wrong detections of angle of arrival (AoA) and angle of departure (AoD), which has a negative effect on the spectral efficiency. In this paper, an enhanced multi-resolution hierarchical codebook design is proposed to realize precise AoD/AoA estimation. First, the necessary number of sampling angles for generating the codebook is given. Then, the algorithm of iterative adjustment (IA) is developed to improve the codebook design. Simulation results show that using the proposed codebook design, the beams can precisely divide the AoA/AoD intervals as the requirements of the adaptive CS based algorithm. Thus, the average angle estimation error is reduced effectively.**

I. Introduction

Thanks to the large available bandwidth, millimeter wave (mmWave) communication technology is promising to meet the demand of significantly increasing data throughput. However, communications at millimeter wave frequency suffer so hostile propagation qualities that a reliable link is difficult to be established. Fortunately, the systems with large scale arrays, which are also called massive multiple-input multiple-output (MIMO) systems, can be employed to produce large beamforming/precoding gain [1]-[3]. Usually, precoding and combining matrices are designed on the basis of complete channel state information (CSI) [4], [5], which includes the knowledge of angle of departure (AoD), angle of arrival (AoA) and complex gain of each path. However, due to the huge training overhead and the small signal-to-noise ratio (SNR) before beamforming, perfect CSI is difficult to be obtained [6]. And the estimation errors of AoDs/AoAs will limit the spectral efficiency.

Substantial researches have been done to realize precise AoD/AoA estimation with a small overhead. Exploiting the sparse feature of mmWave channel, the compressed sensing (CS) based channel estimation methods are developed in [6]-[10]. In [6], based on the efficient and flexible hybrid analog/digital precoding structure, a multi-resolution hierarchical codebook and a hierarchical searching algorithm are proposed. Compared with exhaustive search, hierarchical search needs lower training overhead, but has low array gain in the early training stages. To solve this problem, an effective power allocation scheme has been proposed in [6]. Another method to solve this problem is developed in [7], where a design of beamforming sequence is proposed to strike a balance between minimizing the training overhead and maximizing the array gain. Besides, to improve the angular resolution without changing the physical structure of the array, an angle estimation algorithm based on antenna array with virtual elements is developed in [8]. In addition, Considering the hardware constrains in mmWave systems, hybrid precoder/combiner design for channel estimation is studied in [6], [9], [10].

The performance of hierarchical search is heavily dependent on the codebook design. Perfect codebook design makes beams precisely divide the AoA/AoD intervals as the requirements of searching algorithms. Although the codebook design using the method of least squares in [6] is simple and effective, it is an imperfect one which leads to wrong detections of fixed AoAs and AoDs. Due to this, the angle estimation error is probably larger than the angle resolution (the maximum estimation error) in theory even if there is no hardware constrains and SNR is large enough.

In this paper, we focus on the perfect multi-resolution hierarchical codebook design to reduce the estimation error of AoD/AoA. Our contributions in this paper are listed as follows. i) The influence of the angle estimation error on achievable spectral efficiency is studied first. This shows the importance of reducing angle estimation error. ii) The lower bound of the number of sampling angles for generating the codebook is given, followed by the study of the influence of the angle sampling number on the performance of the codebook. iii) The algorithm of iterative adjustment (IA) is provided to generate the ideal training beams for estimation. The beams optimized by IA can precisely divide the AoA/AoD intervals as the requirements of searching algorithms. Therefore, the angle resolution in theory can be reached in ideal cases.

II. System Model and Adaptive Compressed Sensing Solution of the Millimeter Wave Channel Estimation Problem

A. System Model

Consider the mmWave downlink system model with only one user in [4], [6]. As shown in Fig. 1, N_{t} antennas and $N_{\mathrm{RF}}^{\mathrm{BS}}$ radio frequency (RF) chains are equipped at the base station (BS) while N_{r} antennas and $N_{\mathrm{RF}}^{\mathrm{MS}}$ RF chains are equipped at

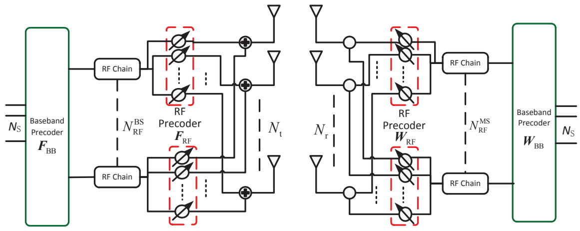

Fig. 1. Transceiver structure at BS and MS.

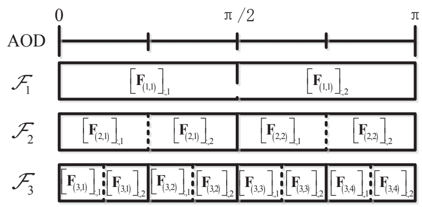

Fig. 2. An example of codebook structure with N=16 and K=2.

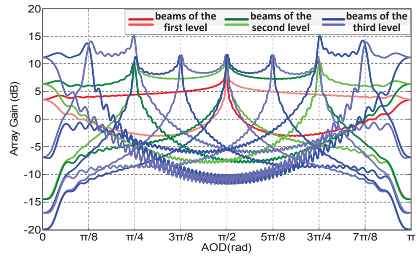

Fig. 3. The array gain of the first three levels with respect to AoD. The codebook design parameters include N=16 and K=2. The number of antenna elements is 64.

the mobile station (MS). BS can send $N_{\rm s}$ data streams to MS, such that $N_{\rm s} \le N_{\rm RF}^{\rm BS} \le N_{\rm t}$ and $N_{\rm s} \le N_{\rm RF}^{\rm MS} \le N_{\rm r}$.

As shown in Fig. 1, the structure of hybrid precoding is adopted. The baseband precoding matrix is $\boldsymbol{F}_{\rm BB} \in \mathbb{C}^{N_{\rm RF}^{\rm BS} \times N_{\rm s}}$, while the RF precoding matrix is $\boldsymbol{F}_{\rm RF} \in \mathbb{C}^{N_{\rm t} \times N_{\rm RF}^{\rm BS}}$ whose entries satisfy $\left|\left[\boldsymbol{F}_{\rm RF}\right]_{m,n}\right|^2 = \frac{1}{N_{\rm t}}$. The precoder at BS is $\boldsymbol{F} = \boldsymbol{F}_{\rm RF}\boldsymbol{F}_{\rm BB}$ that satisfies $\|\boldsymbol{F}\|_{\rm F}^2 = N_{\rm s}$. Similarly, the baseband combining matrix is $\boldsymbol{W}_{\rm BB} \in \mathbb{C}^{N_{\rm RF}^{\rm MS} \times N_{\rm s}}$, while the RF combining matrix is $\boldsymbol{W}_{\rm RF} \in \mathbb{C}^{N_{\rm r} \times N_{\rm RF}^{\rm MS}}$ whose entries satisfy $\left|\left[\boldsymbol{W}_{\rm RF}\right]_{m,n}\right|^2 = \frac{1}{N_{\rm r}}$. The combiner at MS is $\boldsymbol{W} = \boldsymbol{W}_{\rm RF}\boldsymbol{W}_{\rm BB}$ that satisfies $\|\boldsymbol{W}\|_{\rm F}^2 = N_{\rm s}$. Since the RF precoder and combiner are realized by the network of phase shifters, they can adjust only the phase of the signal. Suppose that $\boldsymbol{s}$ is the $N_{\rm s} \times 1$ transmitted symbol vector such that $\mathbb{E}\left[\boldsymbol{s}\boldsymbol{s}^{\rm H}\right] = \frac{1}{N_{\rm s}}\boldsymbol{I}_{N_{\rm s}}$, where $\boldsymbol{I}_N$ denotes an $N \times N$ identity matrix, and $P_{\rm s}$ is the average total transmit power. The received signal observed by MS is

$$\begin{aligned} \boldsymbol{y} &= \sqrt{P_{\rm s}}\boldsymbol{W}_{\rm BB}^{\rm H}\boldsymbol{W}_{\rm RF}^{\rm H}\boldsymbol{H}\boldsymbol{F}_{\rm RF}\boldsymbol{F}_{\rm BB}\boldsymbol{s} + \boldsymbol{W}_{\rm BB}^{\rm H}\boldsymbol{W}_{\rm RF}^{\rm H}\boldsymbol{n} \\ &= \sqrt{P_{\rm s}}\boldsymbol{W}^{\rm H}\boldsymbol{H}\boldsymbol{F}\boldsymbol{s} + \boldsymbol{W}^{\rm H}\boldsymbol{n} \end{aligned} \tag{1}$$

where $\boldsymbol{H} \in \mathbb{C}^{N_{\rm r} \times N_{\rm t}}$ is the channel matrix and $\boldsymbol{n} \sim \mathcal{CN}\left(0, \sigma^2 \boldsymbol{I}_{N_{\rm r}}\right)$ is the additive complex Gaussian noise vector with mean 0 and covariance matrix $\sigma^2\boldsymbol{I}_{N_{\rm r}}$. The two dimension (2D) geometric channel model [4], [6] is adopted in this paper. The channel matrix can be expressed as

$$\boldsymbol{H} = \sqrt{\frac{N_{\rm t}N_{\rm r}}{\rho}} \sum_{l=1}^{L} \alpha_l \boldsymbol{a}_{\rm MS}\left(\theta_l\right)\boldsymbol{a}_{\rm BS}^{\rm H}\left(\varphi_l\right) \tag{2}$$

where L denotes the number of scattering paths, ρ denotes the average path-loss between BS and MS, φ_l, θ_l and α_l denote the AoD, the AoA and the complex gain of the lth path, respectively. The vectors $\boldsymbol{a}_{\rm BS}\left(\varphi_l\right)$ and $\boldsymbol{a}_{\rm MS}\left(\theta_l\right)$ are the array response vectors (ARVs) at BS and MS, respectively. $\boldsymbol{a}_{\rm BS}\left(\varphi_l\right)$ can be expressed as

$$\boldsymbol{a}_{\rm BS}(\varphi_l) = \frac{1}{\sqrt{N_{\rm t}}}\left[1, e^{j(2\pi/\lambda)d\cos\varphi_l}, \cdots, e^{j(2\pi/\lambda)d(N_{\rm BS}-1)\cos\varphi_l}\right] \tag{3}$$

where d is the distance between adjacent antennas and λ denotes the wavelength of the signal. $\boldsymbol{a}_{\rm MS}\left(\theta_l\right)$ can be expressed as the similar fashion. We assume that $d = \frac{\lambda}{2}$ in the following of this paper.

The achievable spectral efficiency of the mmWave channel can be denoted as [4]

$$\begin{aligned} R = \log_2\Bigg(\bigg|\boldsymbol{I}_{N_{\rm s}} + \frac{P_{\rm s}}{\rho N_{\rm s}}\boldsymbol{R}_n^{-1}\boldsymbol{W}_{\rm BB}^{\rm H}\boldsymbol{W}_{\rm RF}^{\rm H}\boldsymbol{H}\boldsymbol{F}_{\rm RF}\boldsymbol{F}_{\rm BB} \\ \times\boldsymbol{F}_{\rm BB}^{\rm H}\boldsymbol{F}_{\rm RF}^{\rm H}\boldsymbol{H}^{\rm H}\boldsymbol{W}_{\rm RF}\boldsymbol{W}_{\rm BB}\bigg|\Bigg) \end{aligned} \tag{4}$$

where $\boldsymbol{R}_n = \sigma_n^2\boldsymbol{W}_{\rm BB}^{\rm H}\boldsymbol{W}_{\rm RF}^{\rm H}\boldsymbol{W}_{\rm RF}\boldsymbol{W}_{\rm BB}$ is the noise covariance matrix after combining. Besides, the signal-to-noise ratio (SNR) in this paper is defined as $\gamma = \frac{P_{\rm s}}{\rho\sigma^2}$.

B. Adaptive Compressed Sensing Based Millimeter Wave Channel Estimation Method

The mmWave channel estimation problem can be formulated as a sparse problem and can be solved by adaptive CS based method, where a multi-resolution hierarchical codebook is needed [6]. An example of the codebook structure with three levels is shown in Fig. 2. And the beams generated by the codebook in Fig. 2 divide the angle intervals as shown in Fig. 3. The AoDs/AoAs are considered to be in the interval of $[0, \pi]$, and this will not influence the recovery of $\boldsymbol{H}$.

The adaptive CS based estimation procedure for single-path channel is briefly described as follows [6]. The AoD/AoA of the path is adaptively detected for several stages. At every stage, the BS uses different training codes in K time slots. The K beams generated by the BS divide the AoD interval selected at the last stage into K partitions uniformly. At the same time, the MS uses K training codes to combine the received signals, and the selected AoA interval is uniformly divided into K partitions similarly. Then the two partitions which are highly likely to respectively contain the AoD and the AoA are selected at MS according to the received signals. The index number of the selected AoD interval is fed back to the BS. In the next stage, the selected AoD and AoA intervals are divided into smaller parts. If the final interval size of $\frac{2\pi}{N}$

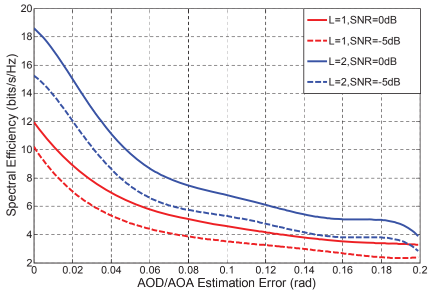

Fig. 4. Achievable spectral efficiency with respect to angle estimation error. The array with 64 antennas is employed both in the BS and the MS.

is required, the final AoD/AoA intervals can be selected after $S = \log_K(N/2)$ stages. Since the AoD/AoA are determined as the central angles of their own final intervals, the angle resolution in theory is π/N. The complex gain of the path can be worked out according to the estimated AoD/AoA. If there are L paths in the channel model, the estimation procedure has L loops. In each loop, the contributions of the paths which have already been estimated should be projected out [6]. We can make N larger than $N_{\rm t}$ to obtain a more precise resolution. However, if beams divide the selected angle intervals unequally, wrong detections will possibly appear.

After channel estimation, the optimal precoder for communication can be obtained through singular value decomposition (SVD) of the channel matrix [4]. And the optimal combiner is designed by minimizing mean square error (MMSE) [4]. As shown in Fig. 4, when the optimal precoder/combiner are used, the achievable spectral efficiency decreases steeply with the increasing of angle estimation error in scenarios of different number of paths and different SNR. Therefore, it is highly significant to reduce the angle estimation error.

III. Enhanced Multi-Resolution Hierarchical Codebook Design

There are two ideas to reduce the angle estimation error. One is increasing estimation stages, which directly increases the angular resolution but has a larger training overhead. The other one is enhancing the codebook design to make beams divide the selected angle intervals uniformly. Since the codebook generation is an off-line work, the additional complexity it brings will not influence the efficiency of estimation. Thus, the second idea is adopted in this paper.

A. How Many Sampling Angles Are Needed?

Take BS as an example to describe the design of multi-resolution hierarchical codebook. And the method of codebook design is also suitable for MS. We use Q as the number of sampling angles for generating a codebook. In the codebook design of [6], Q is exactly the resolution parameter N. What is different from [6] is that Q here can be larger than N.

Based on the codebook design in [6], the question of designing codes of level s and subset k is to solve an overdetermined linear equation set like this

$$\boldsymbol{A}_Q^{\rm H}\boldsymbol{F}_{(s,k)} = C_s\boldsymbol{G}_{(s,k)} \tag{5}$$

where $\boldsymbol{A}_Q = [\boldsymbol{a}_{\rm BS}(\varphi_1), \boldsymbol{a}_{\rm BS}(\varphi_2), \ldots, \boldsymbol{a}_{\rm BS}(\varphi_Q)]$ is the collection of ARVs with $\varphi_u = \frac{2\pi u}{Q}, u = 1, 2, \cdots, Q$, $\boldsymbol{F}_{(s,k)} \in \mathbb{C}^{N_{\rm t}\times K}$ is K codes in subset k, level s, C_s is a constant used to satisfy $\left\|\boldsymbol{F}_{(s,k)}\right\|_{\rm F} = K$, and $\boldsymbol{G}_{(s,k)} \in \mathbb{C}^{Q\times K}$ is a matrix where the mth column contains ones in the locations u, $u \in \boldsymbol{I}_{(s,k,m)}$ and zeros in the locations u, $u \notin \boldsymbol{I}_{(s,k,m)}$. The expression of $\boldsymbol{I}_{(s,k,m)}$ is

$$\begin{aligned}\boldsymbol{I}_{(s,k,m)} = \Big\{ & \frac{Q}{K^s}\left(K(k-1)+m-1\right)+1, \cdots, \\ & \frac{Q}{K^s}\left(K(k-1)+m\right)\Big\}\end{aligned} \tag{6}$$

The method of least squares is employed to solve equations (5) and the result, if exists, can be expressed as [6]

$$\boldsymbol{F}_{(s,k)} = C_s\left(\boldsymbol{A}_Q^{\rm H}\right)^{\dagger}\boldsymbol{G}_{(s,k)} = C_s\left(\boldsymbol{A}_Q\boldsymbol{A}_Q^{\rm H}\right)^{-1}\boldsymbol{A}_Q\boldsymbol{G}_{(s,k)} \tag{7}$$

To guarantee the existence of least squares solutions of codes, the lower bound of sampling angle number Q is given in Lemma 1.

Lemma 1: The necessary condition of the existence of least squares solutions of codes in (7) is

$$Q \geq 2N_{\rm t} - 1 \tag{8}$$

Proof: Apparently, the existence of least squares solution (7) is equivalent to that the matrix $\boldsymbol{A}_Q\boldsymbol{A}_Q^{\rm H}$ is invertible. Then we have $N_t = \operatorname{rank}\left(\boldsymbol{A}_Q\boldsymbol{A}_Q^{\rm H}\right) \leq \operatorname{rank}(\boldsymbol{A}_Q) \leq N_t$. Therefore, if the least squares solution exists, the rank of $\boldsymbol{A}_Q$ must equal to N_t.

We know that $\boldsymbol{A}_Q$ is the collection of ARVs and the $(k+1)$th $(k = 0, 1, \cdots, Q-1)$ column of $\boldsymbol{A}_Q$ is $\boldsymbol{a}_k = \left[1, e^{j\pi\cos(2\pi k/Q)}, \cdots, e^{j\pi(N_t-1)\cos(2\pi k/Q)}\right]^{\rm T}$. Because of the equation $\cos\frac{2\pi k}{Q} = \cos\frac{2\pi(Q-k)}{Q}$, we have $\boldsymbol{a}_k = \boldsymbol{a}_{Q-k}$ when $k \neq 0$. If Q is an even number, since the equation $e^{j\pi} = e^{-j\pi}$, we have $\boldsymbol{a}_0 = \boldsymbol{a}_{Q/2}$. Therefore, there are $Q/2$ different ARVs. If Q is an odd number, there are $\frac{Q+1}{2}$ different ARVs.

If the equation $\operatorname{rank}(\boldsymbol{A}_Q) = N_t$ is true, we have $\frac{Q}{2} \geq N_t$ when Q is even and $\frac{Q+1}{2} \geq N_t$ when Q is odd. Therefore, we get the conclusion that $Q \geq 2N_t - 1$. ■

The inequality (8) is a necessary condition rather than a sufficient condition of the existence the least squares solution for the reason that we cannot guarantee all the different ARVs are linear uncorrelated as the increase of Q. In fact, when the number of antennas is 64 or more, $2N_{\rm t}$ sampling angles are not enough.

Besides satisfying (8), the number of sampling angles should be large enough to provide adequate objects for the method of least squares. The influence of Q is further illustrated in Fig. 5 and Fig. 6. The results are obtained with the parameters $N = 256$, $K = 2$ and $N_{\rm t} = 64$.

The gain curves generated by the codes in subset 10, level 5 with different values of Q are illustrated in Fig. 5. If Q

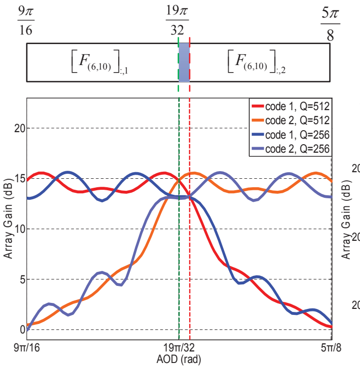

Fig. 5. Array gain curves generated by codes in subset 10, level 5 with the parameters $N_{\rm t} = 64$ and $K = 2$.

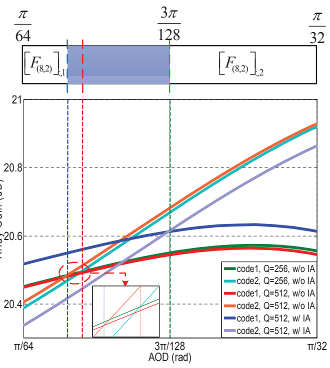

Fig. 6. Array gain curves generated by codes in subset 2, level 7 with the parameters $N_{\rm t} = 64$ and $K = 2$.

equals to 256, the boundary formed by the two beams, which is marked by the red dotted line in Fig. 5, is different from the ideal boundary which is in the center of the selected interval and marked by the green dotted line. This leads to an unequal division of the selected interval. Thus, if the AoD is in the dark blue interval with the width of about 0.01 in Fig. 5, the wrong detection occurs. Unfavorable codes of this kind also exist in other subsets and levels, so the wrong detections exist widely. If Q increases to 512, the actual boundary is exactly the ideal boundary as shown in Fig. 5. The reason is that more objects for least squares are provided by enlarging Q.

However, for some subsets, the performance of least squares cannot be improved by enlarging Q. The codes in subset 2, level 7 are taken as example. The gain curves with different designs are illustrated in Fig. 6. As shown in this figure, without any other measures like IA, even if Q is large enough, there is still an interval between the actual boundary and the ideal boundary. Hence, the resolution in theory is still difficult to reach.

B. *The Algorithm of Iterative Adjustment*

The algorithm of IA is introduced to solve the problem of unequal division of the selected interval. In order to obtain enough degrees of freedom to adjust in the last level, the sampling angle number must be at least $2N$. We use $\delta_m \left(m = 2, \cdots, K\right)$, which is defined as the ratio of the gain of the $(m-1)$th code to the gain of the mth code at the boundary angle, to evaluate the division deviation. If δ_m equals to 1 for any m, the intersection point of any two gain curves lies in the ideal boundary.

The IA algorithm is described as follow. As shown in Algorithm 1, we assume that $\boldsymbol{F} = \boldsymbol{F}_{(s,k)}$ is the original codes in subset k, level s by the method in section A. And $\boldsymbol{G}^{(0)} = \boldsymbol{A}_Q^{\rm H}\boldsymbol{F}^{(0)}$ is the initial gain matrix. Then, a few iterations are carried out. In the pth iteration, for example, the $(K-1)$ gains at the boundary angles are multiplied by their corresponding δ_m. The $(m-1)$th gain value at the boundary angle can be found in the mth column of $\boldsymbol{G}^{(p-1)}$ by an index number which can be expressed as $\tilde{n}_m = (k-1)\cdot\frac{Q}{2^s} + (m-1)\cdot\frac{Q}{2^s K}$. The

Algorithm 1 Iterative Adjustment for Hierarchical Multi-Resolution Codebook

Input: Original codes $\boldsymbol{F}$; ARVs A_Q; Maximum acceptable error ε

Initialization: $\boldsymbol{G}^{(0)} = \boldsymbol{A}_Q^{\rm H}\boldsymbol{F}^{(0)}$; $\boldsymbol{F}^{(0)} = \boldsymbol{F}$

$\delta_1 = 1, \delta_2 = \cdots = \delta_K = 0$; $p = 0$

while $(\exists m, |\delta_m - 1| > \varepsilon)$ **do**

  $p = p + 1$

  for $m = 2$**to**K **do**

    $\delta_m = \left|\left[\boldsymbol{G}^{(p-1)}\right]_{\tilde{n}_m, m-1}\right| / \left|\left[\boldsymbol{G}^{(p-1)}\right]_{\tilde{n}_m, m}\right|$

    $\left[\boldsymbol{G}_{\rm A}^{(p-1)}\right]_{\tilde{n}_m, m} = \left[\boldsymbol{G}^{(p-1)}\right]_{\tilde{n}_m, m} \times \delta_m$

  end for

  $\boldsymbol{G}_{\rm A}^{(p-1)} = \left\{\left[\boldsymbol{G}_{\rm A}^{(p-1)}\right]_{:,1}, \left[\boldsymbol{G}_{\rm A}^{(p-1)}\right]_{:,2}, \cdots, \left[\boldsymbol{G}_{\rm A}^{(p-1)}\right]_{:,K}\right\}$

  $\boldsymbol{F}^{(p)} = \left(\boldsymbol{A}_Q\boldsymbol{A}_Q^{\rm H}\right)^{-1}\boldsymbol{A}_Q\boldsymbol{G}_{\rm A}^{(p-1)}$

  $\boldsymbol{G}^{(p)} = \boldsymbol{A}_Q^{\rm H}\boldsymbol{F}^{(p)}$

end while

Output: $\boldsymbol{F}^* = \left(K / \left\|\boldsymbol{F}^{(p)}\right\|_{\rm F}\right)\boldsymbol{F}^{(p)}$

adjusted gain matrix $\boldsymbol{G}_A^{(p-1)}$ is used to generate $\boldsymbol{F}^{(p)}$. Then, a new gain matrix $\boldsymbol{G}^{(p)}$ is obtained and will be adjusted in the next iteration. The algorithm is carried on until all $|\delta_m - 1|$ are small enough. As shown in Fig. 6, after IA, the actual boundary is exactly the ideal boundary.

The convergence analysis of IA with $K = 2$ is described as follow. In the pth iteration, the evaluation parameter is $\delta^{(p)} = M / \left|\boldsymbol{g}^{(p)}(\tilde{n})\right|$, where $M = \left|\boldsymbol{G}^{(p)}(\tilde{n}, 1)\right|$ is stationary, and $\boldsymbol{g}^{(p)}(\tilde{n}) = \boldsymbol{G}^{(p)}(\tilde{n}, 2)$. After the adjustment, $\boldsymbol{g}_{\rm A}^{(p)} = \boldsymbol{g}^{(p)} + (\delta_p - 1)\,\boldsymbol{g}^{(p)}(\tilde{n})\,\boldsymbol{e}_{\tilde{n}}^{\rm T}$, where $\boldsymbol{e}_{\tilde{n}}$ is a Q-dimensional row vector with one in the location $\tilde{n}$ and zeros in the other locations. Then, in the $(p+1)$th iteration, we have

$$\begin{aligned}\boldsymbol{g}^{(p+1)}(\tilde{n}) &= \boldsymbol{e}_{\tilde{n}}\boldsymbol{g}^{(p+1)} = \boldsymbol{e}_{\tilde{n}}\boldsymbol{A}_Q^{\rm H}\left(\boldsymbol{A}_Q^{\rm H}\right)^{\dagger}\boldsymbol{g}_{\rm A}^{(p)} \\ &= \boldsymbol{g}^{(p)}(\tilde{n}) + \left(\delta^{(p)} - 1\right)\boldsymbol{g}^{(p)}(\tilde{n})\,\boldsymbol{e}_{\tilde{n}}\boldsymbol{A}_Q^{\rm H}\left(\boldsymbol{A}_Q^{\rm H}\right)^{\dagger}\boldsymbol{e}_{\tilde{n}}^{\rm T} \\ &= \left[1 + \left(\delta^{(p)} - 1\right) z_{\tilde{n}}\right]\boldsymbol{g}^{(p)}(\tilde{n})\end{aligned} \tag{9}$$

where $z_{\tilde{n}} = \boldsymbol{e}_{\tilde{n}}\boldsymbol{A}_Q^{\rm H}\left(\boldsymbol{A}_Q\boldsymbol{A}_Q^{\rm H}\right)^{-1}\boldsymbol{A}_Q\boldsymbol{e}_{\tilde{n}}^{\rm T} > 0$ because $\left(\boldsymbol{A}_Q\boldsymbol{A}_Q^{\rm H}\right)^{-1}$ is a positive definite matrix. Hence,

$$\frac{\delta^{(p+1)}}{\delta^{(p)}} = \frac{\left|\boldsymbol{g}^{(p)}(\tilde{n})\right|}{\left|\boldsymbol{g}^{(p+1)}(\tilde{n})\right|} = \frac{1}{1 + \left(\delta^{(p)} - 1\right) z_{\tilde{n}}} \tag{10}$$

We have $\delta^{(p+1)} < \delta^{(p)}$ when $\delta^{(p)} > 1$, as well as $\delta^{(p+1)} > \delta^{(p)}$ when $\delta^{(p)} < 1$. Thus, δ converge to 1 after enough iterations.

The codes in the codebook cannot be used for precoding before they are decomposed into hybrid precoders. The algorithm of orthogonal matching pursuit (OMP) [4] is employed to solve the decomposition problem. In this algorithm, the analog precoding vectors are selected form A_Q. The performance of OMP is poor if there are not enough RF chains.

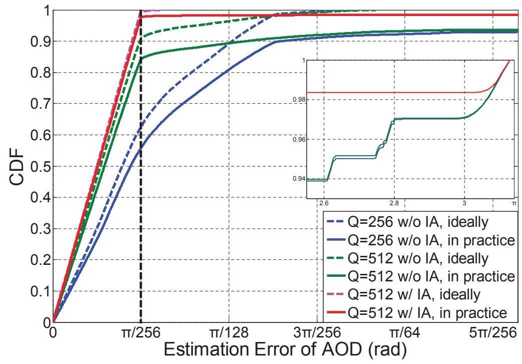

Fig. 7. The CDFs of the AoD estimation error with different codebook designs. The simulation results is obtained in both the ideal case and the practical case with 64 antennas in both the BS and the MS

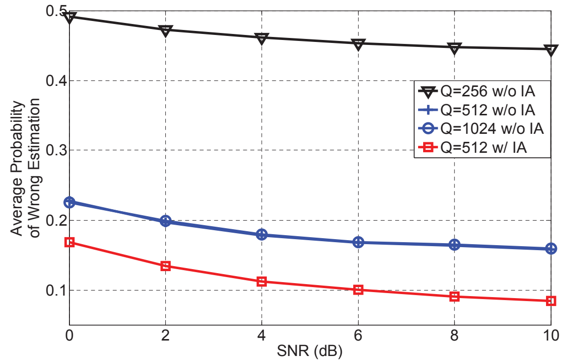

Fig. 8. Average Probability of Wrong Estimation with the parameters $N_t = N_r = 64$ and $N_{\mathrm{RF}}^{\mathrm{BS}} = N_{\mathrm{RF}}^{\mathrm{BS}} = 16$.

IV. Performance Evaluation

Simulation results of channel estimation are given in this part to evaluate the performance of the codebook design. An mmwave system with a single BS-MS downlink is considered. The antenna array with 64 elements and 16 RF chains is equipped both in BS and MS. The channel model is simplified as single-path scenario. If the beams divide angle intervals equally in single-path scenario, they do in multi-path scenario. We assume that the estimation parameters $N = 256$ and $K = 2$, and the transmit power in each stage is equal. The estimation of AoD is taken as an example, and the case is the same for the estimation of AoA.

The cumulative distribution functions (CDFs) of the estimation errors of AoDs with different codebook designs are compared in Fig. 7. In this simulation, we randomly selected 100000 pairs of AoD/AoA. And the results are obtained both in the ideal case, where fully digital structure is employed and no noise exists, and the practical case, where 16 RF chains are employed and the SNR is 10 dB. If the estimation procedure is normal, the largest estimation error is $\pi/256$. The scheme where Q equals to N is the method taken in [6]. As shown in Fig. 7, the enlargement of Q contributes to reducing the estimation error to some extent. When the algorithm of IA is employed, the estimation error is reduced effectively and the angular resolution in theory can be reached in the ideal case. In the practical case, there are a small number of estimation errors of approximately π, which are caused by the back lobes. But they have little impact on the recovery of $\boldsymbol{H}$.

In Fig. 8, the performances of different codebook designs with different SNR values are compared. When the estimation error is larger than the angular resolution in theory, we call this estimation a wrong estimation. The average probability of wrong estimation is defined as $\underset{\theta\in[0,\pi]}{\mathrm{E}}\left[\Pr\left(\left|\theta-\hat{\theta}\right| > \frac{\pi}{256}\right)\right]$, where $\mathrm{E}\left[\cdot\right]$ denotes the averaging function, θ and $\hat{\theta}$ denotes the real AoD and the estimated AoD, respectively. As shown in Fig. 8, the probability of wrong estimation reduced a lot after the enlargement of Q and there is no improvement when we continue to enlarge Q. The employment of the algorithm of IA can reduce the probability of wrong estimation further.

V. Conclusion

In this paper, in order to enhance the multi-resolution hierarchical codebook design, we analyzed the necessary number of sampling angles for generating a codebook and proposed the IA algorithm. The proposed scheme contributes to a more precise AoD and AoA estimation. Thus higher spectrum efficiency can be reached. Simulation results show that the proposed scheme mitigate the average probability of wrong estimation. Hence, the average angle estimation error is reduced. Furthermore, the codebook design method can be employed in the multi-path channel model.

References

[1] J.G. Andrews et al.,"What Will 5G Be?" *IEEE Journal on Selected Areas in Communications*, vol. 32, no. 6, pp. 1065-1082, Jun. 2014.

[2] Z. Pi and F. Khan, "An introduction to millimeter-wave mobile broadband systems," *IEEE Communications Magazine*, vol. 49, no. 6, pp. 101-107, Jun. 2011.

[3] T.E. Bogale and L.B. Le, "Beamforming for multiuser massive MIMO systems: Digital versus hybrid analog-digital," *IEEE Global Communications Conference (GLOBECOM)*, Dec. 2014, pp. 4066-4071.

[4] O.E. Ayach, S. Rajagopal, S. Abusurra, Z. Pi and R.W. Heath, "Spatially Sparse Precoding in Millimeter Wave MIMO Systems," *IEEE Transactions on Wireless Communications*, vol. 13, no. 3, pp. 1499-1513, Mar. 2014.

[5] H.M. kWON, G. Kwon, Y. Shim and H. Park, "Design of Millimeter Wave Hybrid Beamforming Systems," *IEEE Vehicular Technology Conference (VTC Fall)*, Sep. 2014.

[6] A. Alkhateeb, O.E. Ayach, G. Leus and R.W. Heath, "Channel Estimation and Hybrid Precoding for Millimeter Wave Cellular Systems," *IEEE Journal of Selected Topics in Signal Processing*, vol. 8, no. 5, pp. 831-846, Oct. 2014.

[7] S. Noh, M.D. Zoltowski, and D.J. Love, "Multi-Resolution Codebook Based Beamforming Sequence Design in Millimeter-Wave Systems," *IEEE Global Communications Conference (GLOBECOM)*, Dec. 2015.

[8] Y. Peng, Y. Li, and P. Wang, "An Enhanced Channel Estimation Method for Millimeter Wave Systems With Massive Antenna Arrays," *IEEE Global Communications Conference (GLOBECOM)*, Dec. 2015.

[9] S. Payami, M. Shariat, M. Ghoraishi and M. Dianati, "Effective RF codebook design and channel estimation for millimeter wave communication systems," *IEEE International Conference on Communication Workshop (ICCW)*, Jun. 2015.

[10] Z. Xiao, T. He, P. Xia and X.G. Xia, "Hierarchical Codebook Design for Beamforming Training in Millimeter-Wave Communication," *IEEE Transactions on Wireless Communications*, pp. 3380-3392, Jan. 2016.